Novel pyrimidopyrimidine derivatives for inhibition of cellular proliferation and motility induced by h-prune in breast cancer

ARTICLE *in* EUROPEAN JOURNAL OF MEDICINAL CHEMISTRY · AUGUST 2012

Impact Factor: 3.45 · DOI: 10.1016/j.ejmech.2012.08.020 · Source: PubMed

11 AUTHORS, INCLUDING:

Valeria Di Dato
Stazione Zoologica Anton Dohrn di Napoli
13 PUBLICATIONS **171** CITATIONS
SEE PROFILE

Natascia Marino
Indiana University-Purdue University India…
24 PUBLICATIONS **365** CITATIONS
SEE PROFILE

Pasqualino De Antonellis
University of Naples Federico II
21 PUBLICATIONS **411** CITATIONS
SEE PROFILE

Massimo Zollo
University of Naples Federico II
116 PUBLICATIONS **4,141** CITATIONS
SEE PROFILE

European Journal of Medicinal Chemistry 57 (2012) 41–50

Contents lists available at SciVerse ScienceDirect

European Journal of Medicinal Chemistry

journal homepage: http://www.elsevier.com/locate/ejmech

Original article

Novel pyrimidopyrimidine derivatives for inhibition of cellular proliferation and motility induced by h-prune in breast cancer

Antonella Virgilio [a,1], Daniela Spano [b,c,1], Veronica Esposito [a], Valeria Di Dato [b,c], Giuseppe Citarella [a], Natascia Marino [c], Veronica Maffia [c], Daniela De Martino [b,c], Pasqualino De Antonellis [b,c], Aldo Galeone [a], Massimo Zollo [b,c,*]

[a] Dipartimento di Chimica delle Sostanze Naturali, Università degli Studi di Napoli Federico II, Via Domenico Montesano 49, 80131 Naples, Italy
[b] Dipartimento di Biochimica e Biotecnologie Mediche, Università degli Studi di Napoli Federico II, Via Sergio Pansini 5, 80131 Naples, Italy
[c] CEINGE, Centro di Ingegneria Genetica e Biotecnologie Avanzate, Via Gaetano Salvatore 486, 80145 Naples, Italy

ARTICLE INFO

Article history:
Received 9 February 2012
Received in revised form
29 June 2012
Accepted 13 August 2012
Available online 23 August 2012

Keywords:
h-Prune
Breast cancer
cAMP
Phosphodiesterase
Cellular motility

ABSTRACT

The human (h)-prune protein is a member of the DHH protein superfamily and it has a cAMP phosphodiesterase activity. Its overexpression in breast, colorectal and gastric cancers correlates with depth of invasion and a high degree of lymph-node metastasis. One mechanism by which h-prune stimulates cell motility and metastasis processes is through its phosphodiesterase activity, which can be suppressed by dipyridamole, a pyrimido[5,4-*d*]pyrimidine analogue. To obtain new and more potent agents that have high specificity towards inhibition of this h-prune activity, we followed structure–activity-relationship methodologies starting from dipyridamole and synthesised eight new pyrimido–pyrimidine derivatives. We analysed these newly generated compounds for specificity towards h-prune activities *in vitro* in cellular models using scintillation proximity assay for cAMP-PDE activity, cell index in cell proliferation assays and transwell methodology for two-dimensional cell migration in a top-down strategy of selection. Our findings show that two pyrimido[5,4-*d*]pyrimidine compounds are more effective than dipyridamole in two highly metastatic cellular models of breast cancer *in vitro*. Future studies will assess their therapeutic effectiveness against breast and other cancers where there is over-expression of h-prune, and in *ad-hoc*, proof of concept, animal models.

1. Introduction

Breast cancer is the most common cancer among women and is a primary cause of cancer death worldwide. Breast cancer is a complex and heterogeneous disease as it comprises multiple tumour entities, that are associated with distinctive histological patterns and different biological features and clinical behaviour. Furthermore, evidence from gene expression microarrays studies has suggested the presence of multiple molecular subtypes of breast cancer that might respond in different ways to different therapies [1]. In breast cancer, metastatic spread is responsible for virtually all of the deaths. About 6% of patients with newly diagnosed disease present with advanced or metastatic breast cancer (MBC), with some 40% of patients who initially present with localised disease eventually progressing to MBC. MBC is a heterogeneous disease that has a clinical behaviour that can be difficult to predict [2]. The choice of treatment is based on patient characteristics (e.g., age), the presence of comorbidities, and/or the previous treatments. In addition, physicians rely on prognostic and predictive targets for therapy, the most established of which are the expression of the oestrogen receptor (ER), progesterone receptor (PR), and human epidermal growth factor receptor-2 (HERB-2) by the tumour tissue. These characteristics help in determining the most effective therapy for an individual patient with MBC [2,3].

Unfortunately, the heterogeneity of the disease and the variability in the individual presentation make the selection of widely accepted patient-specific treatment guidelines difficult. For these reasons, clinicians must determine which therapeutic intervention might be most appropriate for each patient, based on individual aspects of the patient clinical profile, and the number and sites of metastases, vital organ involvement and previous disease-free survival interval [3]. Thus, new therapeutic interventions have

Abbreviations: MBC, metastatic breast cancer; PDE, phosphodiesterase; DP, dipyridamole; CI, cell index; MTS, 3-(4,5-dimethylthiazol-2-yl)-5-(3-carboxymethoxyphenyl)-2-(4-sulfophenyl)-2*H*-tetrazolium.

* Corresponding author. CEINGE, Biotecnologie Avanzate SCARL, Via Gaetano Salvatore 486, 80145 Napoli, Italy. Tel.: +39 081 3737 875; fax: +39 081 3737 711.
E-mail address: massimo.zollo@unina.it (M. Zollo).

[1] These two authors contributed equally to the work.

0223-5234/$ – see front matter © 2012 Elsevier Masson SAS. All rights reserved.
http://dx.doi.org/10.1016/j.ejmech.2012.08.020

the need for new classes of inhibitors [4]. However, despite significant progress in the detection and treatment of breast cancer, MBC remains incurable. The treatment goals for MBC are therefore focussed on prolonging patient survival and providing palliative control of symptoms.

Metastasis is a highly complex molecular and cellular process, during which cancer cells escape from the original tumour tissue, invade the surrounding tissues of the primary tumour, penetrate the lymphatic system or a blood vessel through which they travel to distal sites, extravasate, and then colonize a second organ [5,6]. Increased invasiveness of cancer cells is a critical step in tumour metastasis and this requires many intracellular and extracellular changes; e.g., cancer cells loosen their adhesion to neighbouring cells and the extracellular matrix, degrade adjacent tissues, and show increased motility [7].

In previous studies, the enzymatic activity of the human (h)-prune protein was shown to be involved in metastasis formation in breast cancer [8]. The h-prune protein is a member of the DHH (Asp–His–His) protein superfamily, and it has a phosphodiesterase (PDE) activity, with a preferential affinity for cAMP over cGMP [8], and an exopolyphosphatase activity, with a preferential affinity for short-chain inorganic polyphosphates over long-chain inorganic polyphosphates [9]. Over-expression of h-prune in the MDA-MB-435 breast cancer cell line promotes cell motility. Consistent with these observations, over-expression of h-prune in breast cancer is correlated with cancer progression and aggressiveness [10,11]. These pro-motility effects of h-prune seen *in vitro* are also significantly associated with lymph-node status (N2–N3) and metastasis formation (M1) *in vivo*, thus indicating that h-prune is a marker of advanced-stage disease status in breast carcinoma [11]. Interestingly, h-prune PDE activity is enhanced by interaction with nm23-H1, and a direct correlation between increased h-prune cAMP-PDE activity and cellular motility has been shown in the breast cancer model [8].

To identify the physiological role of h-prune, several known selective PDE inhibitors were tested for their ability to affect h-prune cAMP-PDE activity. Among these, dipyridamole (DP) emerged as the most active in inhibiting the cAMP-PDE activity of h-prune purified protein, expressed by Baculovirus Expression system, with an IC_{50} of 0.78 μM [8]. To develop a therapeutic programme aimed at identifying new, more potent and selective, compounds that can inhibit this h-prune activity, we undertook the preparation of new molecules based on the pyrimido[5,4-*d*]pyrimidine aromatic heterocycle characteristic of DP. We performed various enzymatic and biological assays to assess the efficacy of the new pyrimido[5,4-*d*]pyrimidine compounds towards the impairing of the h-prune PDE activity and cell migration and proliferation, with the final goal being to identify a candidate molecule for *in vivo* testing for anti-cancer properties against metastatic breast cancer.

2. Results

2.1. Development and selection of pyrimido[5,4-d]pyrimidine derivatives that inhibit h-prune cAMP-PDE activity

As there is no detailed information concerning the full structure of the h-prune protein and the site of action of DP that would allow us to use molecular modelling techniques, we decided to prepare a series of novel eight pyrimido[5,4-*d*]pyrimidine derivatives and, then, test them by suitable biological assays considering the potential of inhibition of the two main functions of h-prune described: (i) increased cAMP-PDE activity in breast cancer cells due to over-expression of h-prune; (ii) enhanced cell migration due to over-expression of h-prune [8].

The new pyrimido[5,4-*d*]pyrimidine derivatives have been designed taking into account the biochemical properties of DP (whose chemical structure is shown in Fig. 1A) and other similar derivatives (DP analogues), properly developed as inhibitors of the nucleoside transport [12,13]. Although the usefulness of DP as inhibitor of the nucleoside transport has been confirmed in *in vitro* experiments, its efficacy and that of some of its derivatives is dramatically reduced in presence of the α_1-acid glycoprotein (an acute phase protein, whose plasma levels can be elevated in cancer patients) due to the ability of DP to bind avidly to it [12,13]. Most importantly, in a structure–activity-relationships study involving 96 compounds [13], authors observed that the influence of the α_1-acid glycoprotein on the activity of most of the molecules investigated was less pronounced than that observed for DP, in compounds bearing a substituted benzylamino group at the pyrimido[5,4-*d*]pyrimidine 4,8-positions. Taking into consideration these data, we have designed 8 new compounds (Fig. 1A–B) that can be considered derivatives of compound **1** characterized by the same groups in 2,6-positions as DP and 4-methoxybenzylamino groups in 4,8-positions that, in several compounds, have proven to impair the binding to α_1-acid glycoprotein.

Previous studies showed DP inhibits the ability of h-prune purified protein to hydrolyze cAMP with an IC_{50} of 0.78 μM [8]. Therefore, firstly we assessed the ability of compound **1** to inhibit the cAMP-PDE activity of h-prune purified protein and determined its IC_{50} value using a scintillation proximity assay. As shown in Supplementary Figure 1, compound **1** inhibited the cAMP-PDE activity of h-prune purified protein with an IC_{50} measured value of 0.21 μM. This value is lower if compared to the DP IC_{50} value, thus indicating compound **1** is more efficient than DP in inhibiting h-prune cAMP-PDE activity and retains a higher specificity towards h-prune cAMP-PDE activity.

The synthesis of the 8 new compounds derived from the compound **1** was performed by following a two steps literature procedure starting from the tetrachloropyrimidopyrimidine [12,13] (Fig. 1C). In this series, most of the substituents R maintain the same number of bonds between the nitrogen atom and a hydroxyl group, as for DP and compound **1**. However, in this case, for several substituents, the flexibility of this part of the molecule has been decreased by introducing cyclic hydroxylamine moieties in order to limit the conformational freedom of the –OH group, in the hypothesis that it is essential for the interaction of the molecule with h-prune. Furthermore, when chiral amines were utilized, pure enantiomers were preferentially used. To evaluate the ability of these new molecules (Fig. 1A–B) to inhibit the h-prune protein directly in a cellular environment, h-prune PDE activity assays were performed on a protein extract from cells over-expressing h-prune and treated with these compounds. For this assay, a stable clone over-expressing h-prune cDNA was expressly created and its cellular properties were determined. The MDA435-C100 cell line was used to generate this stable clone that over-expressed h-prune, following a previously described methodology of transfection and stable clone selection [8]. This stable breast cancer clone was then assessed for expression of h-prune by western blotting using an anti-h-prune antibody (Fig. 2A). The parental cell line containing the empty vector plasmid was used as control. Protein extracts from the stable clone line (MDA435-c100-h-prune) were assessed after treatment with 1 μM of these compounds, as described in the Material and Methods.

As a useful comparison, the PDE activity of DP and compound **1**, from which the series of compounds originated, was also evaluated using the same assay. As discussed above, this experiment was performed using whole protein extracts of cell line MDA435 over-expressing h-prune protein and not using the h-prune purified protein as previously carried out in D'Angelo and collaborators [8]. For these reasons the dipyridamole induced-inhibition of h-prune

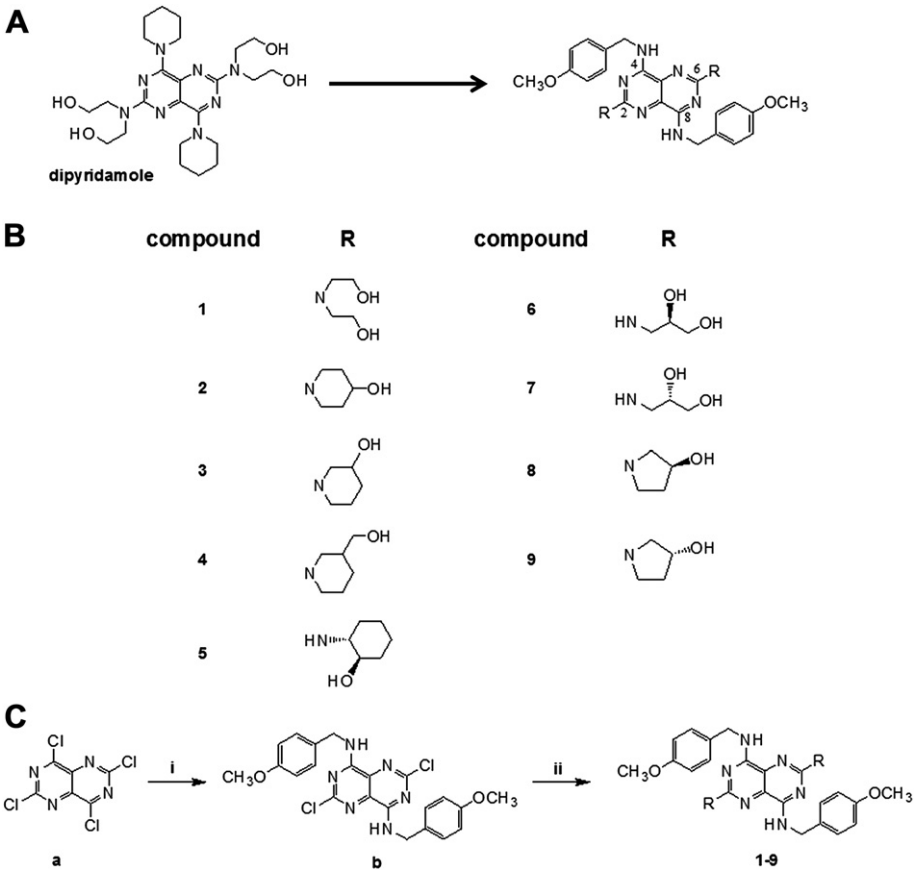

Fig. 1. Chemical structures (A and B) and synthetic strategy (C) of the pyrimido[5,4-*d*]pyrimidine derivatives investigated. Reagents and conditions: (i) 4-methoxybenzylamine, K_2CO_3, THF (solvent), r.t.; (ii) appropriate 1° or 2° amine, 100–150 °C.

cAMP-PDE activity in a cellular environment was found lower if compared to previously data obtained on h-prune purified protein [8]. The results point to an increased activity for all compounds **2**–**9** in comparison with DP and their precursor **1** (Fig. 2B).

2.2. Inhibition of cell proliferation by the newly generated pyrimido [5,4-d]pyrimidine derivatives

To further study the efficacy of our here identified compounds we decided to follow a "Top-Down" strategy. We have used the next two biological functions (cellular proliferation and cellular motility) related to h-prune activity in tumorigenic cells to further screen the newly generated compounds. For this reason we decided to follow through the analyses above presented a next series of assays to select the best compound using structure–activity-relationship approach. As a crucial feature of cancer cells is their high proliferation rate, we assessed the inhibition of cell proliferation by these new compounds. The cells used as cellular model were MDA-MB-231T, which express high level of h-prune (Fig. 3A). Based on the cAMP-PDE activity assays results, we focused our attention on

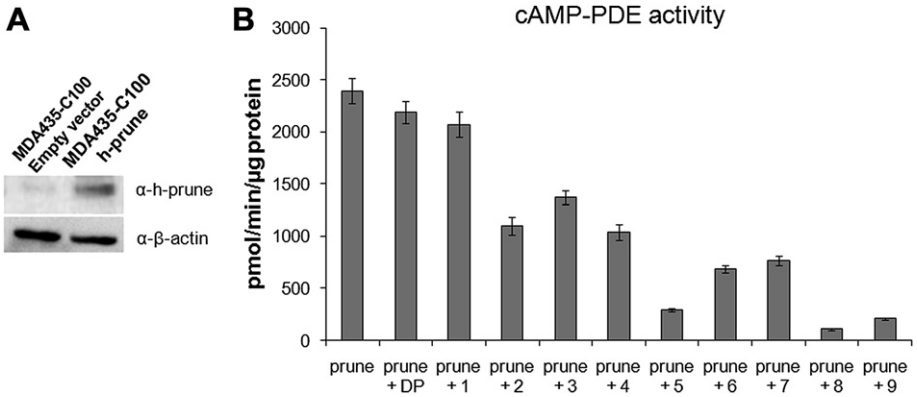

Fig. 2. Efficacy of pyrimido[5,4-*d*]pyrimidine derivatives in inhibiting h-prune cAMP-PDE activity. (A) Characterization of h-prune over-expressing MDA435-C100 clone. Immunoblotting analysis of h-prune protein expression was performed on total protein extracts from MDA435-C100 empty vector and h-prune over-expressing clones. β-actin was used as a control for equal loading. (**B**) cAMP-PDE activity assay was performed on protein extracts from MDA435-C100 h-prune over-expressing clone treated with vehicle, dipyridamole (DP) or pyrimido[5,4-*d*]pyrimidine derivatives. Data are means ± standard errors (SE). A representative experiment of two performed with similar results is shown.

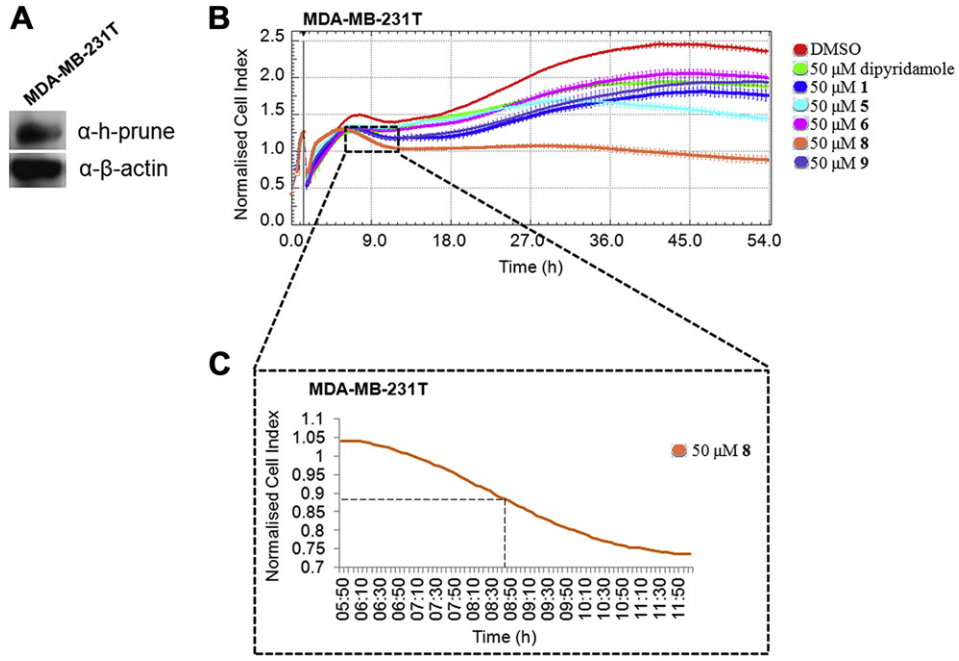

Fig. 3. Efficacy of pyrimido[5,4-*d*]pyrimidine derivatives in inhibiting cell proliferation. (A) Immunoblotting analysis of h-prune protein expression was performed on total protein extracts from MDA-MB-231T cells. β-actin was used as a control for equal loading. (B) Dynamic monitoring of MDA-MB-231T cell proliferation in response to 50 μM DP and other compounds. In the graph the black line shows the time of drug addition at which the CI values were normalised. A representative experiment of two performed with similar results is shown. Data are means ± standard deviation (SD). (C) Enlargement of the dynamic monitoring of MDA-MB-231T cell proliferation in response to 50 μM compound **8**. The inflection point of the curve indicates the time where 50 percent inhibition of proliferation is achieved by using 50 μM compound **8**.

compounds **5**, **6**, **8** and **9** and evaluated their ability to impair cell proliferation in the MDA-MB-231T proliferation assay in real time (xCelligence System).

Previous studies showed that 20 μg/ml DP (corresponding to a final of 40 μM concentration) inhibits cell growth [14]. Additionally in our recently published data we found that the concentration of DP able to significantly impair cell proliferation, in breast cancer cell lines, corresponds to 50 μM [15]. Therefore we decide to assay DP and the pyrimido[5,4-*d*]pyrimidine derivatives, including compound **1**, at the concentration of 50 μM. As shown in Fig. 3B, MDA-MB-231T cells treated with DP and the other pyrimido[5,4-*d*] pyrimidine derivatives did not show any significant changes in the cell index (CI), as a measure of cell proliferation, during the first 5 h of their addition. After this time, there was a significant lower increase in the CI values of treated cells compared to vehicle (DMSO)-treated cells. These data show that compound **1** blocked cell proliferation more effectively than DP at the same molar concentration (Fig. 3B). Inhibition of cell proliferation by compound **5** was comparable to that of DP during the first 27 h of treatment, although at longer times of treatment compound **5** showed greater inhibition than DP (Fig. 3B). For compounds **6** and **9**, inhibition of cell proliferation remained generally similar to that of DP throughout the assay period. In contrast, compound **8** was much more efficient than DP in inhibiting cell proliferation throughout the remaining assay period (Fig. 3B). Comparison of the effects on cell proliferation of the most efficient compounds with inhibition of the h-prune cAMP-PDE activity, showed that the inhibition for compound **8** in the cell proliferation assay increases relative to DP from 9 h to around 45 h of incubation, as there is no further increase in CI seen with compound **8**. In contrast, in comparison with DP, the smaller anti-proliferative effects of compound **9** are lost over the next 30 h of treatment (Fig. 3B). A comparison of the chemical structure of compounds **8** and **9** shows that they differ only in the spatial orientation of the –OH group in the R substituent (Fig. 1B). Although this structural difference has a negligible effect on the inhibition of h-prune cAMP-PDE activity by compounds **8** and **9** (Fig. 2), the different spatial orientation of the –OH group appears to have an important role in their inhibition of cell proliferation, with compound **8** more efficient than compound **9**. For a direct comparison of the proliferation inhibition of these compounds, we compared the CI after 24 h of treatment. As shown in Table 1, compound **8** impaired cell proliferation more effectively than the other compounds. The time-course analysis of cell proliferation in presence of 50 μM compound **8** showed that the 50% inhibition of proliferation, measured as CI value, is achieved 7 h and 20 min after drug addition (which was performed at 1 h and 27 min from cell proliferation experiment start) (Fig. 3C and Table S1). Furthermore, only the compounds **1**, **8** and **9** showed a statistically significant decrease in CI values at 24 h treatment compared to DP (Table 1). *In vitro* proliferation assays in presence of two different concentrations of compounds **8** and **9** were also performed to evaluate the dose–response effects on inhibiting cell proliferation. As showed in the upper and bottom panels of Fig. 4A, the increase of compounds concentration caused an increase of their proliferation inhibitory effects. We compared the CI curves of

Table 1
Cell index values from the in real time cell proliferation assays after 24 h of treatment.

Drugs	CI 24 h after drugs addition	SE	*p* value of compound vs DP
DMSO	1.777	0.000	–
DP	1.472	0.008	–
1	1.185	0.028	0.0006
5	1.407	0.030	0.1336
6	1.452	0.025	0.5496
8	0.770	0.016	<0.0001
9	1.239	0.035	0.0026

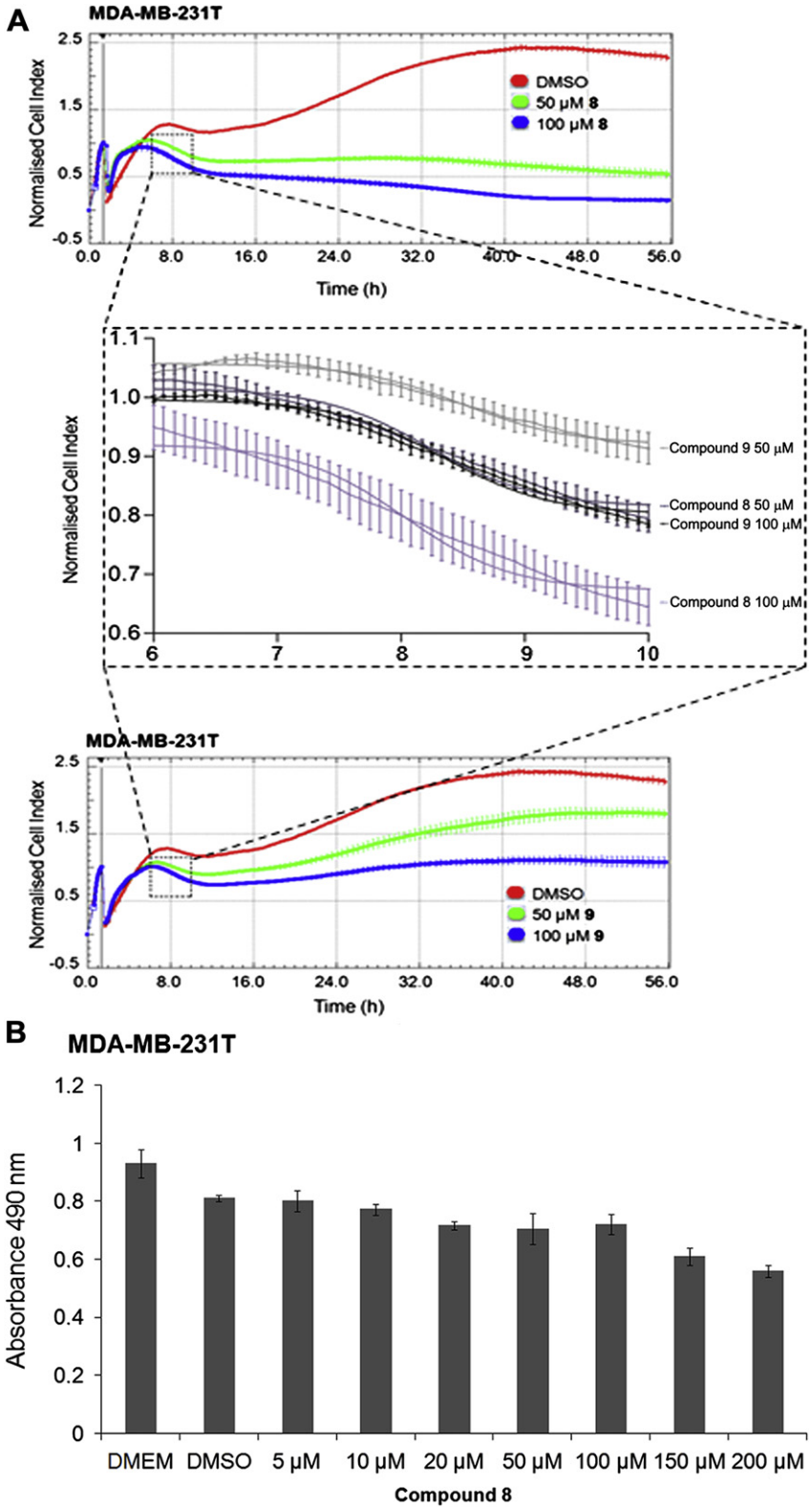

Fig. 4. Dose–response curves of compounds **8** and **9**. (A) The graphs show the dynamic monitoring of MDA-MB-231T cell proliferation in response to the DMSO control (0) and 50 μM and 100 μM of compounds **8** (upper panel) and **9** (bottom panel). Black marker line is the time of compound addition to which CI values were normalised. Data are means ± SD. For each panel, a representative experiment of two independent *in vitro* proliferation assays performed with similar results is shown. Middle panel is an enlargement of the dynamic monitoring assays shown in upper and bottom panels within the time window of 6–10 h. (B) Representative end-point cell proliferation assay (of two experiments performed with similar results) with MDA-MB-231T cells treated with DMSO (control) or compound **8** (as indicated). Data are means ± SE.

compounds **8** and **9**, at 50 and 100 μM concentrations and normalised at time of drug addition, within the time window of 6–10 h (see middle panel of Fig. 4A). The corresponding single curves within this time window are shown in Supplementary Figure 2. This comparison showed that the inhibition of cell proliferation induced by compound **9** at 100 μM concentration was comparable to that obtained by compound **8** at 50 μM concentration (Fig. 4A middle panel). These data overall are indicating that: (i) the compound **8** is more potent than compound **9** on impairing cell proliferation and (ii) the compound **9** needs higher concentrations to achieve the same effect on cellular proliferation in comparison of compound **8**. For this reason the higher potency of compound **8** may explain its efficacy on inhibiting cell proliferation over compound **9**. Furthermore, as shown in Table 2, evaluating over the time cell proliferation inhibition (at the time of 15, 20, 30 and 40 h), we found that the 100 μM concentration used for compound **9** was not able to inhibit the cell proliferation in comparison of compound **8** used instead at 50 μM. It should be noted that while compound **8**, during the time of in real time proliferation assay, is able to impair the cellular proliferation (measured as CI values) (see data at 15 h 0.73–0.52; at 20 h 0.74–0.48; at 30 h 0.77–0.37; at 40 h 0.68–0.22), compound **9** is performing with less efficacy, thus showing a potential high grade of degradation within the cell, being the CI values increased within the time of treatment (see data in Table 2). Indeed a sign of potential degradation into the cell was observed (see data at 15 h: 0.94–0.76; at 20 h: 1.04–0.82; at 30 h: 1.42–1.01; at 40 h: 1.70–1.09). Overall these data show lower potency and efficacy of compound **9** compared to compound **8**, and allow us to conclude that this latest is more effective and potent than compound **9** on inhibiting cell proliferation. Then to further confirm this dose-dependent inhibition of cell proliferation induced by the compound **8**, we performed end-point cell proliferation assays (MTS assays) in a range of compound **8** concentrations. As previously already shown, this assay confirmed that the compound **8** inhibited the cellular proliferation of MDA-MB-231T breast cancer cells in a dose-dependent inhibition (Fig. 4B).

2.3. Inhibition of cell motility by the newly generated pyrimido[5,4-d] pyrimidine derivatives

Previous reports have shown that h-prune over-expression in the MDA-MB-435 breast cancer cell line promotes cell motility [8] and is correlated with breast cancer progression and aggressiveness [10,11]. To investigate the ability of these new pyrimido[5,4-*d*] pyrimidine derivatives to inhibit cell motility, we performed *in vitro* cell motility assay on the MDA-MB-231T metastatic breast cancer cells [16]. We analysed inhibition of cell motility by the four best compounds in the PDE-activity assay, namely **5**, **6**, **8**, **9** and **1** and DP for comparison at a concentration of 8 μM. As shown in Fig. 5A, the inhibition of cellular motility of the compound **1** was slightly greater with respect to DP. However, among the new derivatives generated from compound **1**, the best one for the inhibition of cell motility was compound **9**. In this case, the different spatial orientation of the –OH group in compounds **8** and **9** (see Fig. 1B) appeared to have an important role against cell motility in this MDA-MB-231T breast cancer model (see Fig. 5A, in the "cell 2D migration assay").

Table 2
Cell index values from the in real time cell proliferation assays in presence of compounds **8** and **9** at the indicated time points.

Time-interval (h)	50 μM compound **8**		100 μM compound **8**		50 μM compound **9**		100 μM compound **9**	
	CI	SE	CI	SE	CI	SE	CI	SE
15	0.73	0.016	0.52	0.024	0.94	0.013	0.76	0.006
20	0.74	0.011	0.48	0.024	1.04	0.022	0.82	0.010
30	0.77	0.021	0.37	0.020	1.42	0.042	1.01	0.021
40	0.68	0.029	0.22	0.008	1.70	0.050	1.09	0.029

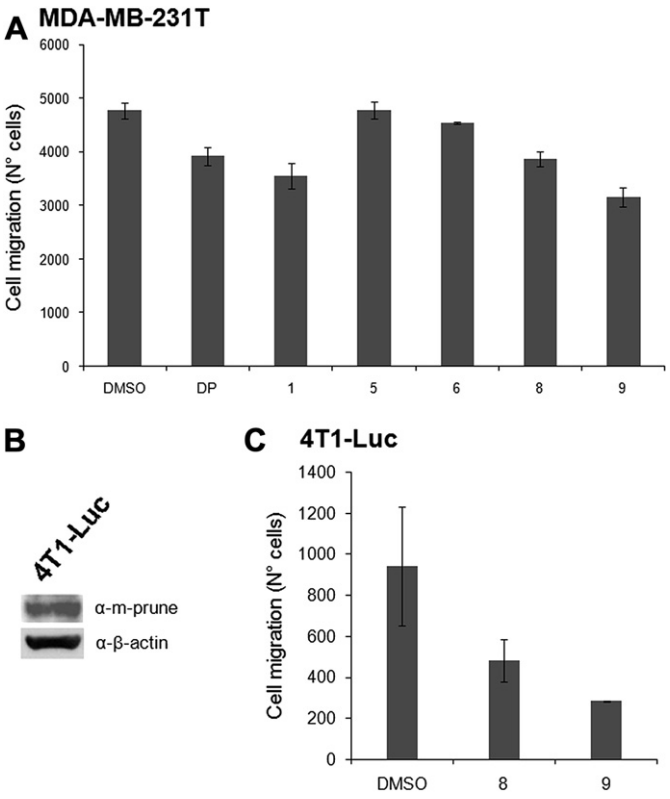

Fig. 5. Efficacy of pyrimido[5,4-*d*]pyrimidine derivatives in inhibiting cell motility. (A) Motility assays were performed on MDA-MB-231T cells treated with vehicle (DMSO), DP or the other compounds at a concentration of 8 μM. Data are means ± SE. A representative experiment of two independent cell motility assays performed with similar results is shown. (B) M-prune endogenous expression in 4T1-Luc cells. Immunoblotting analysis of m-prune protein expression performed on total protein extracts from 4T1-Luc cells. β-actin was used as a control for equal loading. (C) Motility assays were performed on 4T1-Luc cells treated with vehicle (DMSO), compounds **8** and **9** at a concentration of 8 μM. Data are means ± SE. A representative experiment of two independent cell motility assays performed with similar results is shown.

It should be noted here that the cell motility process is affected by cytoskeleton rearrangements due to assembly of F-actin and its polymerization and depolarization in focal adhesions. This function is regulated by h-prune in a context of the interactions and regulation of additional protein partners (e.g. GSK-3β) and by the specific cAMP-PDE activity of h-prune [17]. However, these are not the only factors that can influence cell motility. This would thus explain the different relative behaviours of compounds **5** and **6** in those PDE assays (Fig. 2B) and cell motility assays (Fig. 5A).

These data indicate that compound **9** can impair cell motility in this two-dimensional (2D) cell migration assay (MDA-MB-231T breast cancer model) with a greater efficacy compared to compound **8**, which was similar to DP to impair cell motility. To further validate this, we evaluated the ability of these compounds to reduce cell motility in an additional model of breast cancer in mouse, the 4T1-Luc cell metastatic model [18], which express a sustained high level of the murine prune homologue (Fig. 5B). As shown in Fig. 5C, both compounds **8** and **9** at a concentration of 8 μM inhibited this 4T1-Luc two-dimensional (2D) migration ability compared to DMSO.

3. Discussion

Our structure–activity-relationship approach here has been valuable for the identification of new molecules that can impair h-prune cAMP-PDE activity and the increased cellular motility in these highly metastatic models of breast cancer. Through the combination of these assays, we have identified two compounds that show increases on their anti-cancer properties, as measured through inhibition of cellular proliferation and motility of these highly metastatic tumours cell lines. Future studies will be directed to the characterization of the site of interaction between h-prune and these newly generated inhibitors. We envision the use of nuclear magnetic resonance (NMR) studies for the identification of the small-molecule binding site and for the optimization of the inhibitor properties [19,20] and thus following studies on RTKs c-Met inhibitors as reviewed by Accornero et al., 2010 [21]. Thus, future NMR studies performed on the pyrimido[5,4-*d*] pyrimidine compounds generated in the present study should provide insights into their interaction with the h-prune binding pocket, and thus will allow the design and the synthesis of further analogues to provide more potent compounds around those scaffolds. In particular, the identification of the h-prune region that interacts with these new pyrimido[5,4-*d*]pyrimidine compounds will provide further insights into the molecular mechanisms underlying their ability to impair h-prune function in cancer.

It is known that h-prune regulates cell motility by two different means of action: through its cAMP-PDE activity and through its interactions with various protein partners, which include nm23-H1 [8,22], GSK-3β [17], paxillin [17], vinculin [17], and ASAP1 [23]. H-prune, GSK-3β, paxillin, vinculin and ASAP1 are all localised within focal adhesions. In particular, a role for h-prune and GSK-3β in the regulation of the disassembly of focal adhesions, to promote cell migration, has been demonstrated [17]. However, if all of these proteins form a unique molecular complex or whether the h-prune interaction with its protein partners is mutually exclusive has not yet been determined. The h-prune region involved in the interaction with its protein partners was previously determined only for nm23-H1 and GSK-3β [24]; studies to resolve the region of protein–protein binding site(s) of h-prune with its other protein partners are ongoing in our laboratory. Moreover, the role of each protein interaction for the promotion of cell motility has not yet been determined. The ability of DP to impair h-prune-induced cell motility has been ascribed to its properties as an inhibitor of the cAMP-PDE activity of h-prune [8], whereas DP did not affect the subcellular localisation of h-prune, indicating that the PDE activity is not required for the localisation of h-prune to focal adhesions [17]. In the future, we will determine which function of h-prune is abrogated by these newly generated pyrimido[5,4-*d*]pyrimidine compounds, and if these compounds can impair protein function through the binding of h-prune with its other protein partners in the focal adhesions compartments.

Questions are raised at this stage about the anti-proliferative properties of those newly identified compounds. We have already shown an anti-proliferative effect of DP [8], as have Curtin and colleagues [25]. At this time, we cannot be certain whether the molecular mechanism underlying those biological effects of DP is the same as these newly identified small molecules. In particular, these molecules can mimic metabolites (purine and pyrimidines) and might have effects on DNA synthesis, acting against *de novo* purine–pyrimidine biosynthesis and potentially being antagonists of nucleotide transport in DNA synthesis. Curtin NJ and colleagues [25] showed that pyrimido[5,4-*d*]pyrimidines act as anti-metabolites, although they were designed as anti-cancer agents, and they still represent a major class with wide therapeutic applications today. Salvage of extracellular purine or pyrimidine nucleosides or bases constitutes an intrinsic resistance mechanism to anti-metabolite inhibitors of *de novo* purine or pyrimidine biosynthesis [26,27]. The pyrimido–pyrimidine cardiovascular agent DP inhibits equilibrative nucleoside transporters [28–30]. Several studies have shown that DP significantly increases the cytotoxic and anti-tumour activity of a variety of inhibitors of *de novo* nucleotide synthesis by blocking the uptake of nucleosides for salvage [31–39]. Moreover, by blocking nucleoside efflux, DP can also exacerbate antifolate-induced nucleotide pool imbalances and increase the cytotoxicities of these inhibitors. These anti-tumour activities and all the other properties of these pyrimido[5,4-*d*] pyrimidines derivatives will be investigated in our future studies.

Recently, some novel pyrimido[5,4-*d*]pyrimidines were efficiently synthesized and evaluated for antibacterial activity against *Mycobacterium tuberculosis* strain H_{37}Rv [40]. Additionally, a patent deposited in USA (US 2003229051, 2003) shows pyrimido[5,4-*d*] pyrimidines derivatives as irreversible inhibitors of tyrosine kinases and their potential use in cancer and in the treatment of inflammatory diseases, such atherosclerosis, restenosis, endometriosis and psoriasis. These data make our newly discovered anti-h-prune derivatives very attractive for testing of their anti-inflammatory properties. Future studies will address these topics.

4. Conclusion

In this study we identified new molecules that can impair h-prune cAMP-PDE, cellular proliferation and increased cellular motility in breast cancer metastatic models. Both the newly identified compounds **8** and **9** are useful targets for future studies that will mainly address their properties as anti-cancer (anti-metastatic) and potentially being new anti-inflammatory candidate molecules as being h-prune involved in those several mechanism functionally related.

5. Experimental protocols

5.1. Synthetic procedures and materials and methods

The general synthetic strategy used to prepare the investigated compounds (**1**–**9**) was similar to that proposed by Curtin et al. [13] in which the preparation of several substituted pyrimido[5,4-*d*] pyrimidines was described (Fig. 1B). General procedure for the first reaction: the 4-methoxybenzylamine (1.1 ml, 8 mmol) was added to a stirred solution of 2,4,6,8-tetrachloropyrimido[5,4-*d*]pyrimidine (a) (490 mg, 1.80 mmol) in dry THF (12 mL) containing K_2CO_3 (1.8 g, 13.5 mmol). The reaction mixture was stirred (1 h) at room temperature under dry conditions until TLC analysis confirmed the absence of starting materials. H_2O (20–30 mL) was added, the reaction mixture was stirred for 20 min, and the precipitated solid was collected by filtration. Chromatography on silica afforded the intermediate compound 2,6-dichloro-4,8-dibenzylaminopyrimido [5,4-*d*]pyrimidine (b) (yields 98%). For the second reaction, intermediate b (0.1–1 mmol) was dissolved in an excess (1–5 mL) of the required amine, and the mixture was stirred at 100–150 °C, until TLC analysis confirmed the absence of starting materials (typically 24–48 h). After the mixture was cooled, the crude product was precipitated by addition of H_2O (30–50 mL) and collected by filtration and/or extraction with EtOAc. The product was purified by chromatography on silica (yields 97%).

^{1}H and ^{13}C NMR spectra were acquired on a Varian Unity Inova700 spectrometer and the residual solvent signal or TMS were used as an internal standard. Spectra were recorded in DMSO-d_6 as solvent. NH signals appeared as broad singlets exchangeable with D_2O. MS (ESI+) was recorded with an API-2000 triple quadrupole mass spectrometer equipped with a turbo ion-spray source

(Applied Biosystem; Thornhill, ON, Canada). NMR and MS experiments were performed at "Centro di Servizi Interdipartimentale di Analisi Strumentale", Università degli Studi di Napoli Federico II. TLC was performed on silica gel 60 plates (Merck, precoated), with $CHCl_3$/MeOH as a mobile phase and was visualized with UV light at 254 and 365 nm. Chromatography was conducted on silica gel (Kieselgel 60, 70–230 mesh). All reagents were purchased from Aldrich Chemical Co. and were used without further purification.

*5.1.1. 1,1′-(4,8-bis(4-Methoxybenzylamino)pyrimido[5,4-d] pyrimidine-2,6-diyl)dipiperidin-4-ol (**2**)*

^{1}H NMR δ 1.30 (4H, 2× C*H*CH$_2$NCH$_2$C*H*), 1.74 (4H, 2× C*H*CH$_2$NCH$_2$C*H*), 3.13 (4H, 2× C*H*NC*H*), 3.67 (2H, CH$_2$N(CH$_2$)$_3$C*H*OH), 3.71 (6H, 2× ArOC*H*$_3$), 4.34 (4H, 2× C*H*NC*H*), 4.56 (4H, 2× C*H*$_2$Ar), 4.66 (2H, 2× O*H*), 6.86 (4H, 4× Ar–*H*), 7.30 (4H, 4× Ar–*H*); ^{13}C NMR δ 4 × 36.1, 4 × 44.4, 2 × 44.5, 2 × 55.1, 2 × 67.6, 4 × 113.7, 4 × 129.2, 2 × 131.9, 2 × 134.0, 2 × 155.0, 2 × 157.7, 2 × 158.3; MS ESI (*m*/*z*): $C_{32}H_{40}N_8O_4$ 601 $(M + H)^+$.

*5.1.2. 1,1′-(4,8-bis(4-Methoxybenzylamino)pyrimido[5,4-d] pyrimidine-2,6-diyl)dipiperidin-3-ol (diastereomeric mixture) (**3**)*

^{1}H NMR δ 1.45 (2H, 2× NCH$_2$C*H*CH$_2$CH(OH)), 1.52 (2H, 2× NCH$_2$CH(OH)C*H*), 1.55 (2H, 2× NCH$_2$C*H*CH$_2$CH(OH)), 1.77 (2H, 2× NCH$_2$CH(OH)C*H*), 3.50 (4H, 2× NC*H*$_2$CH$_2$), 3.57 (4H, 2× NC*H*$_2$CHOH), 3.72 (6H, 2× ArOC*H*$_3$), 4.35 (2H, 2× NCH$_2$C*H*(OH)CH$_2$), 4.61 (4H, 2× C*H*$_2$Ar), 4.81 (2H, 2× O*H*), 6.88 (4H, 4× Ar–*H*), 7.34 (4H, 4× Ar–*H*), 6.81 (2H, 2× N*H*); ^{13}C NMR δ 2 × 23.9, 2 × 33.1, 2 × 44.4, 2 × 46.1, 2 × 53.5, 2 × 55.1, 2 × 66.3, 4 × 113.7, 4 × 129.2, 2 × 131.9, 2 × 134.0, 2 × 155.0, 2 × 157.7, 2 × 158.3; MS ESI (*m*/*z*): $C_{32}H_{40}N_8O_4$ 601 $(M + H)^+$.

*5.1.3. (1,1′-(4,8-bis(4-Methoxybenzylamino)pyrimido[5,4-d] pyrimidine-2,6-diyl)bis(piperidine-3,1-diyl))dimethanol (diastereomeric mixture) (**4**)*

^{1}H NMR δ 1.23 (2H, 2× NCH$_2$CH(CH$_2$OH)C*H*CH$_2$), 1.39 (2H, 2× NCH$_2$C*H*CH$_2$), 1.56 (2H, 2× NCH$_2$C*H*CH$_2$), 1.67 (2H, 2× NCH$_2$CH(CH$_2$OH)C*H*CH$_2$), 1.76 (2H, 2× NCH$_2$C*H*(CH$_2$OH)), 2.67 (2H, 2× NC*H*(CH$_2$)$_2$), 2.89 (2H, 2× NC*H*(CH$_2$)$_2$), 3.34 (4H, 2× C*H*$_2$OH), 3.34 (4H, 2× NHC*H*$_2$CH(CH$_2$OH)), 3.71 (6H, 2× ArOC*H*$_3$), 4.58 (4H, 2× C*H*$_2$Ar), 4.66 (2H, 2× O*H*), 6.86 (4H, 4× Ar–*H*), 7.34 (4H, 4× Ar–*H*); ^{13}C NMR δ 2 × 25.6, 2 × 27.7, 2 × 39.4, 2 × 44.4, 2 × 46.6, 2 × 49.7, 2 × 55.1, 2 × 65.4, 4 × 113.7, 4 × 129.2, 2 × 131.9, 2 × 134.0, 2 × 155.0, 2 × 157.7, 2 × 158.3; MS ESI (*m*/*z*): $C_{34}H_{44}N_8O_4$ 629 $(M + H)^+$.

*5.1.4. (1R,1′R,2R,2′R)-2,2′-(4,8-bis(4-Methoxybenzylamino) pyrimido[5,4-d]pyrimidine-2,6-diyl)bis(azanediyl)dicyclohexanol (**5**)*

^{1}H NMR δ 1.09 (2H, 2× (NH)CHCH(OH)C*H*), 1.13 (2H, 2× (NH) CHCH$_2$C*H*), 1.19 (2H, 2× (NH)CHC*H*(CH$_2$)$_3$), 1.20 (2H, 2× (NH) CH(CH$_2$)C*H*), 1.61 (2H, 2× (NH)CHC*H*(CH$_2$)$_3$), 1.62 (2H, 2× (NH) CH(CH$_2$)C*H*), 1.66 (2H, 2× (NH)CHCH$_2$C*H*), 1.78 (2H, 2× (NH) CHCH(OH)C*H*), 2.72 (2H, 2× (NH)C*H*), 3.38 (2H, 2× (NH) CHC*H*(OH)), 3.72 (6H, 2× ArOC*H*$_3$), 4.0 (2H, 2× (NH)CH), 4.62 (4H, 2× C*H*$_2$Ar), 4.81 (2H, 2× O*H*), 6.86 (4H, 4× Ar–*H*), 7.30 (4H, 4× Ar–*H*), 7.40 (2H, 2× N*H*CH$_2$Ar); ^{13}C NMR δ 2 × 24.8, 2 × 25.0, 2 × 33.8, 2 × 34.4, 2 × 44.4, 2 × 55.1, 2 × 56.9, 2 × 75.6, 4 × 113.7, 4 × 129.2, 2 × 131.9, 2 × 134.0, 2 × 155.0, 2 × 157.7, 2 × 158.3; MS ESI (*m*/*z*): $C_{34}H_{44}N_8O_4$ 629 $(M + H)^+$.

*5.1.5. (2R,2′R)-3,3′-(4,8-bis(4-Methoxybenzylamino)pyrimido[5,4-d] pyrimidine-2,6-diyl)bis(azanediyl)dipropane-1,2-diol (**6**) and (2S,2′S)-3,3′-(4,8-bis(4-methoxybenzylamino)pyrimido[5,4-d] pyrimidine-2,6-diyl)bis(azanediyl)dipropane-1,2-diol (**7**)*

^{1}H NMR δ 3.20 (2H, 2× NHC*H*), 3.35 (2H, 2× NHCH$_2$C*H*OH), 3.35 (2H, 2× NHCH$_2$CHOHC*H*OH), 3.42 (2H, 2× NHC*H*), 3.62 (2H, 2× NHCH$_2$CHOHC*H*OH), 3.72 (6H, 2× ArOC*H*$_3$), 4.49 (4H, 2× C*H*$_2$Ar), 4.57 (2H, 2× CH$_2$O*H*), 4.72 (2H, 2× CHO*H*), 5.91 (2H, 2× N*H*CH$_2$CHOHCH$_2$OH), 6.87 (4H, 4× Ar–*H*), 7.29 (4H, 4× Ar–*H*), 7.51 (2H, 2× N*H*CH$_2$Ar); ^{13}C NMR δ 2 × 44.4, 2 × 44.9, 2 × 55.1, 2 × 63.9, 2 × 72.7, 4 × 113.7, 4 × 129.2, 2 × 131.9, 2 × 134.0, 2 × 155.0, 2 × 155.4, 2 × 158.3; MS ESI (*m*/*z*): $C_{28}H_{36}N_8O_6$ 581 $(M + H)^+$.

*5.1.6. (3S,3′S)-1,1′-(4,8-bis(4-Methoxybenzylamino)pyrimido[5,4-d]pyrimidine-2,6-diyl)dipyrrolidin-3-ol (**8**) and (3R,3′R)-1,1′-(4,8-bis(4-methoxybenzylamino)pyrimido[5,4-d]pyrimidine-2,6-diyl) dipyrrolidin-3-ol (**9**)*

^{1}H NMR δ 1.86 (2H, 2× NCH$_2$C*H*CH(OH)), 1.98 (2H, 2× NCH$_2$C*H*CH(OH)), 3.55 (4H, 2× NC*H*$_2$CH$_2$), 3.57 (4H, 2× NC*H*$_2$CH(OH)), 3.71 (6H, 2× ArOC*H*$_3$), 4.35 (2H, 2× NCH$_2$C*H*(OH)), 4.61 (4H, 2× C*H*$_2$Ar), 4.99-5.10 (2H, 2× O*H*), 6.88 (4H, 4× Ar–*H*), 7.34 (4H, 4× Ar–*H*); ^{13}C NMR δ 2 × 44.4, 2 × 44.5, 2 × 54.8, 2 × 55.1, 2 × 69.4, 2 × 79.3, 4 × 113.7, 4 × 129.2, 2 × 131.9, 2 × 134.0, 2 × 155.0, 2 × 157.7, 2 × 158.3; MS ESI (*m*/*z*): $C_{30}H_{36}N_8O_4$ 573 $(M + H)^+$.

5.2. Cell culture

MDA-435-C100 empty vector and h-prune over-expressing cells were obtained as previously described [8]. MDA-435-C100 stable clones, mouse mammary gland tumour cell line 4T1-Luc and human mammary gland tumour cell line MDA-MB-231T were grown in high glucose Dulbecco's modified Eagle's medium (DMEM; Invitrogen) supplemented with 10% (v/v) foetal bovine serum (Invitrogen), 2 mM L-Glutamine (Invitrogen), and 1% (v/v) antibiotics (10,000 U/ml penicillin, and 10 mg/ml streptomycin (Invitrogen)). The cells were grown at 37 °C in a humidified atmosphere of 95% air and 5% CO_2 (v/v).

5.3. Immunoblotting

Total protein extracts from cells were prepared and used for immunoblotting as previously described [8] using the A59 rabbit anti-prune antibody, and detected by a horseradish peroxidase–conjugated anti-rabbit (1:3000) antibody (Amersham). A mouse anti-β-actin antibody (1:5.000; Sigma–Aldrich) was used as the loading control.

5.4. Protein expression and purification in Baculovirus

Protein expression was performed using Baculovirus expression system as previously described [8].

5.5. Characterization of the pyrimido[5,4-d]pyrimidine derivatives action on h-prune PDE activity

For the determination of the ability of compound **1** to inhibit the h-prune purified protein cAMP-PDE activity scintillation proximity assays were performed as previously described [8] using the Phosphodiesterase [^{3}H]cAMP SPA enzyme assay (Amersham), according to the manufacturer's protocol. In particular, 400 ng of purified enzymes were incubated for 15 min at 30 °C in a reaction mix containing 50 mM Tris–HCl pH 7.5, 8.3 mM $MgCl_2$, 1.7 mM EGTA, 0.005 μCi/μl [^{3}H]cAMP in presence of increasing concentrations of compound **1** (0.0001 μM, 0.0001 μM, 0.001 μM, 0.01 μM, 0.2 μM, 0.4 μM, 0.8 μM, 1.6 μM, 3.2 μM, 6.4 μM, 10 μM). The reactions were terminated by adding 50 μl of Yttrium SPA PDE beads and mixed well to redistribute the settled beads and allowed to stand at room temperature for 20 min. The reactions were counted on a scintillation counter. All reactions, including buffer-only blanks, were conducted in triplicate. Enzyme activities were

calculated according to the amount of radio-labelled product detected, according to the manufacturer's protocol. The IC_{50} was determined by plotting log compound **1** concentration on X-axis and % cAMP-PDE inhibition on Y-axis. The percentage inhibition curves were plotted using four determinations. The IC_{50} value was calculated by using Sigmoidal dose–response (Prism Release 5.04; GraphPad Software Inc, USA). A total of two independent sets of experiments were performed.

Cellular extracts were prepared to measure h-prune PDE activity. Briefly the MDA435-C100 cells over-expressing h-prune were plated onto 6-well dishes with 2 ml growth medium/well the day before treatment. After 24 h, the medium was replaced with fresh medium containing the vehicle (DMSO or PEG/PBS) or the indicated compound at 1 μM concentration, and the cells were incubated over night at 37 °C 5% CO_2. Treated and untreated cells were washed three times with ice-cold phosphate-buffered saline and lysed with lysis buffer (50 mM Tris–HCl, pH 7.4, 1% Nonidet P40, 0.25% sodium deoxycholate, 150 mM NaCl, 1 mM EDTA, 1 mM phenylmethylsulfonyl fluoride, 1 mM Na_3VO_4, 1 mM NaF, 1 mM benzamidine, 1 μg/ml aprotinin, and 1 μg/ml leupeptin) at 4 °C. The lysates were incubated in ice for 30 min and then centrifuged at 14,000 g for 10 min. The protein concentrations of the resulting supernatants were determined using the Bradford protein assay (Bio-Rad Laboratories, Hercules, CA). Equal amounts of whole protein extract were used for the cAMP-PDE assays, using the Phosphodiesterase [^{3}H]cAMP SPA enzyme assay (Amersham), according to the manufacturer's protocol. Briefly, total protein extracts were diluted as required and assessed in a 100 μl reaction mix containing 50 mM Tris–HCl pH 7.5, 8.3 mM $MgCl_2$, 1.7 mM EGTA, 0.005 μCi/μl [^{3}H]cAMP. Reactions were incubated for 15 min at 30 °C, then terminated by adding 50 μl of Yttrium SPA PDE beads and mixed well to redistribute the settled beads and allowed to stand at room temperature for 20 min. The reactions were counted on a scintillation counter. All reactions, including buffer-only blanks, were conducted in triplicate. Enzyme activities were calculated according to the amount of radio-labelled product detected, according to the manufacturer's protocol. A total of two independent sets of experiments were performed.

5.6. 2D cell migration assays

100,000 MDA-MB-231T cells, resuspended in serum free medium (200 μl) in the presence of DMSO (control) or each specific compound at a concentration of 8 μM, were plated in triplicate into the upper chamber of an 8 μm pore size 24 well-plates Transwell insert (Corning Incorporated, Costar, Corning, NY, USA). Complete medium (600 μl) containing 0.5% FBS, as chemoattractant, and DMSO (control) or each specific compound at a concentration of 8 μM was added to the lower chamber. The 4T1-luc migration assay was performed as described with a few changes: 25,000 cells were seeded in the upper chamber; the low chamber contained complete medium supplemented with 10% FBS. MDA-MB-231T cells were lived to migrate for 3 h at 37 °C 5% CO_2, while the 4T1-Luc cells were lived to migrate for 4 h at 37 °C 5% CO_2. After migration cells were fixed with 2.5% glutaraldehyde and stained in Gill's Hematoxilin No.1.

Each of the triplicate chamber was divided in nine fields. A picture of each field was taken from optical microscopy and migrating cells were counted by using Cell Counter ImageJ program.

As control of normal migration, the experimental point "Not Treated" (only the DMEM growth medium) was settled down. Each compound was then compared to the Placebo (DMSO 0.001%) experimental point, as a control of their dissolving solution, and to the DP experimental point to identify the pyrimido[5,4-*d*] pyrimidine derivative with the best migration inhibitory activity. A total of two independent experiments was performed.

5.7. xCelligence system

The Real-Time Cell Analysis (RTCA) Instrument (Roche) uses an xCelligence system which is based on the RT-CES (Real-Time Cell Electronic Sensor) system, that allows label-free dynamic monitoring of cell proliferation and viability in real time [41,42]. Briefly, this system uses an electronic readout of impedance to non-invasively quantify adherent cell proliferation and viability in real-time. The cells are seeded into standard microtiter plates that contain microelectronic sensor arrays. The interactions of the cells with the electronic biosensors generate a cell-electrode impedance response that not only indicates the cell viability, but also correlates with the number of cells seeded in the well. Cell-sensor impedance is expressed as an arbitrary unit called the Cell Index (CI) [41,42]. The cell culture conditions on the sensor device are the same as those in the tissue disks described above. For real-time calculations of the CI during the *in vitro* proliferation assay, the background impedance of each sensor well of the E-plate 16 (ACEA Biosciences, Inc) was measured in the absence of cells. To do this, 40 μl cell culture media was added into each well for the baseline measurements, followed by addition of the cells to the sensor wells (20,000 MDA-MB-231T cells/well). Four replicates for each experimental point were used, so four single readings of CI from four different wells for each experimental point were obtained. After cell seeding, the sensor device was left at room temperature for 30 min to reduce the variability resulting from edge effects [43], then it was put into the RTCA Instrument inside a 37 °C, 5% CO_2 incubator and the CI of each well was monitored automatically with the xCelligence system software. To ensure consistent initial cell conditions for the proliferation assays, each independent compound or DMSO (placebo) were added once after the CI reached a range of 1.0–1.2, indicating 50%–60% cell confluence. After addition of the compounds or DMSO, the plate with the cells was mounted back into the RTCA Instrument inside a 37 °C, 5% CO_2 incubator. The CI was automatically and continuously monitored by xCelligence system software every 5 min for up to 54–56 h. Furthermore *in vitro* proliferation assays in real-time were performed in presence of 50 and 100 μM compounds **8** and **9** to valuate dose–response effects in inhibiting cell proliferation. A total of two independent experiments was performed.

5.8. End-point proliferation assay (MTS assays)

Proliferation assays were performed using the CellTiter 96 Aqueous One Solution Cell Proliferation Assay (Promega). 10^4 MDA-MB-231T cells/well were plated into 96-well plates and treated with DMSO (control) or DMSO containing compound **8** (at the indicated concentrations) for 24 h. Each experimental point was assessed in quadruplicate. For each experimental point, 20 μl (3-(4,5-dimethylthiazol-2-yl)-5-(3-carboxymethoxyphenyl)-2-(4-sulfophenyl)-2*H*-tetrazolium) (MTS) solution (1.90 mg/ml) was added to each well, and the cells were incubated for 2 h at 37 °C. Absorbance was then measured at 490 nm using a microtiter plate reader (VICTOR3 1420 Multilabel Counter, Perkin Elmer). For each experimental point, the means of absorbance and their standard errors (SE) were calculated. A total of two independent sets of experiments were performed.

5.9. Statistical analysis

The statistical comparison of the data from the *in vitro* treatments was performed using Students' *t* test. Statistical significance was established at $p \leq 0.05$.

Disclosure: The authors declare that they have no competing interests as defined by European Journal of Medicinal Chemistry, or

other interests that might be perceived to influence the results and discussion reported in this paper.

Acknowledgements

We would like to thank N.J. Curtin and R.J. Griffin at AICR-UK (New Castle, UK) for valuable discussions about strategies to develop new anti-h-prune compounds.

This work was supported by the following grants: FP6-EET pipeline LSH-CT-2006-037260 (MZ), FP7-Tumic HEALTH-F2-2008-201662 (MZ), Associazione per la Ricerca sul Cancro AIRC (MZ), Associazione Italiana contro la lotta al Neuroblastoma (MZ), PRIN-MIUR PRIN (E5AZ5F) 2008 (MZ). Legge n.5, Regione Campania 2007-8 (MZ). Valeria Di Dato and Daniela Spano were supported by Fondazione San Paolo University of Naples, Federico II, DBBM. Veronica Maffia, Natascia Marino, Pasquale De Antonellis were supported by EET-pipeline LSH-CT-2006-037260 and Tumic HEALTH-F2-2008-201662). Daniela De Martino is supported by Associazione Italiana contro la lotta al Neuroblastoma (MZ).

Appendix A. Supplementary data

Supplementary data related to this article can be found at http://dx.doi.org/10.1016/j.ejmech.2012.08.020.

References

[1] B. Weigelt, J.S. Reis-Filho, Histological and molecular types of breast cancer: is there a unifying taxonomy? Nat. Rev. Clin. Oncol. 6 (2009) 718–730.
[2] E. Andreopoulou, G.N. Hortobagyi, Prognostic factors in metastatic breast cancer: successes and challenges toward individualized therapy, J. Clin. Oncol. 26 (2008) 3660–3662.
[3] C. Bernard-Marty, F. Cardoso, M.J. Piccart, Facts and controversies in systemic treatment of metastatic breast cancer, Oncologist 9 (2004) 617–632.
[4] J. O'Shaughnessy, Extending survival with chemotherapy in metastatic breast cancer, Oncologist 10 (2005) 20–29.
[5] D. Spano, C. Heck, P. De Antonellis, G. Christofori, M. Zollo, Molecular networks that regulate cancer metastasis, Semin Cancer Biol. 22 (2012) 234–249.
[6] D. Spano, M. Zollo, Tumor microenvironment: a main actor in the metastasis process, Clin Exp Metastasis 4 (2012) 381–395.
[7] P.S. Steeg, Tumor metastasis: mechanistic insights and clinical challenges, Nat. Med. 12 (2006) 895–904.
[8] A. D'Angelo, L. Garzia, A. André, P. Carotenuto, V. Aglio, O. Guardiola, G. Arrigoni, A. Cossu, G. Palmieri, L. Aravind, M. Zollo, Prune cAMP phosphodiesterase binds nm23-H1 and promotes cancer metastasis, Cancer Cell. 5 (2004) 137–149.
[9] M. Tammenkoski, K. Koivula, E. Cusanelli, M. Zollo, C. Steegborn, A.A. Baykov, R. Lahti, Human metastasis regulator protein H-prune is a short-chain exo-polyphosphatase, Biochemistry 47 (2008) 9707–9713.
[10] A. Forus, A. D'Angelo, J. Henriksen, G. Merla, G.M. Maelandsmo, V.A. Florenes, S. Olivieri, B. Bjerkehagen, L.A. Meza-Zepeda, F. del Vecchio Blanco, C. Muller, F. Sanvito, J. Kononen, J.M. Nesland, O. Fodstad, A. Reymond, O.P. Kallioniemi, G. Arrigoni, A. Ballabio, O. Myklebost, M. Zollo, Amplification and over-expression of PRUNE in human sarcomas and breast carcinomas-a possible mechanism for altering the nm23-H1 activity, Oncogene 20 (2001) 6881–6890.
[11] M. Zollo, A. Andre, A. Cossu, M.C. Sini, A. D'Angelo, N. Marino, M. Budroni, F. Tanda, G. Arrigoni, G. Palmieri, Overexpression of h-prune in breast cancer is correlated with advanced disease status, Clin. Cancer Res. 11 (2005) 199–205.
[12] H.C. Barlow, K.J. Bowman, N.J. Curtin, A.H. Calvert, B.T. Golding, B. Huang, P.J. Loughlin, D.R. Newell, P.G. Smith, R.J. Griffin, Resistance-modifying agents. Part 7: 2,6-disubstituted-4,8-dibenzylaminopyrimido[5,4-*d*]pyrimidines that inhibit nucleoside transport in the presence of alpha1-acid glycoprotein (AGP), Bioorg. Med. Chem. Lett. 10 (2000) 585–589.
[13] N.J. Curtin, H.C. Barlow, K.J. Bowman, A.H. Calvert, R. Davison, B.T. Golding, B. Huang, P.J. Loughlin, D.R. Newell, P.G. Smith, R.J. Griffin, Resistance-modifying agents. 11. (1) Pyrimido[5,4-*d*]pyrimidine modulators of antitumor drug activity. Synthesis and structure-activity relationships for nucleoside transport inhibition and binding to alpha1-acid glycoprotein, J. Med. Chem. 47 (2004) 4905–4922.
[14] N. Van Larebeke, C. Dragonetti, M. Mareel, Effect of dipyridamole on invasion of five types of malignant cells in organ culture, Clin. Exp. Metastasis 7 (1989) 645–657.
[15] D. Spano, J.C. Marshall, N. Marino, D. De Martino, A. Romano, M. N. Scoppettuolo, A. M. Bello, V. Di Dato, L. Navas, G. De Vita, C. Medaglia, P.S. Steeg and M. Zollo. Dipyridamole prevents triple-negative breast-cancer progression. Clin. Exp. Metastasis. (in press).
[16] M. Deckers, M. van Dinther, J. Buijs, I. Que, C. Löwik, G. van der Pluijm, P. ten Dijke, The tumor suppressor Smad4 is required for transforming growth factor beta-induced epithelial to mesenchymal transition and bone metastasis of breast cancer cells, Cancer Res. 66 (2006) 2202–2209.
[17] T. Kobayashi, S. Hino, N. Oue, T. Asahara, M. Zollo, W. Yasui, A. Kikuchi, Glycogen synthase kinase 3 and h-prune regulate cell migration by modulating focal adhesions, Mol. Cell. Biol. 26 (2006) 898–911.
[18] K. Tao, M. Fang, J. Alroy, G.G. Sahagian, Imagable 4T1 model for the study of late stage breast cancer, BMC Cancer 8 (2008) 228.
[19] T. Diercks, M. Coles, H. Kessler, Applications of NMR in drug discovery, Curr. Opin. Chem. Biol. 5 (2001) 285–291.
[20] H.O. Villar, J. Yan, M.R. Hansen, Using NMR for ligand discovery and optimization, Curr. Opin. Chem. Biol. 8 (2004) 387–391.
[21] P. Accornero, L.M. Pavone, M. Baratta, The scatter factor signaling pathways as therapeutic associated target in cancer treatment, Curr. Med. Chem. 17 (25) (2010) 2699–2712, Review.
[22] L. Garzia, A. D'Angelo, A. Amoresano, S.K. Knauer, C. Cirulli, C. Campanella, R.H. Stauber, C. Steegborn, A. Iolascon, M. Zollo, Phosphorylation of nm23-H1 by CKI induces its complex formation with h-prune and promotes cell motility, Oncogene 27 (2008) 1853–1864.
[23] T. Müller, U. Stein, A. Poletti, L. Garzia, M. Rothley, D. Plaumann, W. Thiele, M. Bauer, A. Galasso, P. Schlag, M. Pankratz, M. Zollo, J.P. Sleeman, ASAP1 promotes tumor cell motility and invasiveness, stimulates metastasis formation in vivo, and correlates with poor survival in colorectal cancer patients, Oncogene 29 (2010) 2393–2403.
[24] N. Marino, M. Zollo, Understanding h-prune biology in the fight against cancer, Clin. Exp. Metastasis 24 (2007) 637–645.
[25] H.D. Thomas, K. Saravanan, L.Z. Wang, M.J. Lin, J.S. Northen, H. Barlow, M. Barton, D.R. Newell, R.J. Griffin, B.T. Golding, N.J. Curtin, Preclinical evaluation of a novel pyrimidopyrimidine for the prevention of nucleoside and nucleobase reversal of antifolate cytotoxicity, Mol. Cancer Ther. 8 (2009) 1828–1837.
[26] J.A. Belt, N.M. Marina, D.A. Phelps, C.R. Crawford, Nucleoside transport in normal and neoplastic cells, Adv. Enzym. Regul. 33 (1993) 235–252.
[27] J. Walling, From methotrexate to pemetrexed and beyond. A review of the pharmacodynamic and clinical properties of antifolates, Invest. New Drugs 24 (2006) 37–77.
[28] S.A. Baldwin, J.R. Mackey, C.E. Cass, J.D. Young, Nucleoside transporters: molecular biology and implications for therapeutic development, Mol. Med. Today 5 (1999) 216–224.
[29] A.M. Wright, W.P. Gati, A.R. Paterson, Enhancement of retention and cytotoxicity of 2-chlorodeoxyadenosine in cultured human leukemic lymphoblasts by nitrobenzylthioinosine, an inhibitor of equilibrative nucleoside transport, Leukemia 14 (2000) 52–60.
[30] W. Schaper, Dipyridamole, an underestimated vascular protective drug, Cardiovasc. Drugs Ther. 19 (2005) 357–363.
[31] J.L. Grem, Biochemical modulation of fluorouracil by dipyridamole: preclinical and clinical experience, Semin. Oncol. 19 (1992) 56–65.
[32] S.B. Howell, D. Hom, R. Sanga, J.S. Vick, I.S. Abramson, Comparison of the synergistic potentiation of etoposide, doxorubicin, and vinblastine cytotoxicity by dipyridamole, Cancer Res. 49 (1989) 3178–3183.
[33] N. Ramu, A. Ramu, Circumvention of adriamycin resistance by dipyridamole analogues: a structure–activity relationship study, Int. J. Cancer 43 (1989) 487–491.
[34] N.L. Lehman, P.V. Danenberg, Modulation of RTX cytotoxicity by thymidine and dipyridamole in vitro: implications for chemotherapy, Cancer Chemother. Pharmacol. 45 (2000) 142–148.
[35] J.A. Nelson, S. Drake, Potentiation of methotrexate toxicity by dipyridamole, Cancer Res. 44 (1984) 2493–2496.
[36] P.B. Desai, R. Sridhar, Potentiation of cytotoxicity of mitoxantrone toward CHO-K1 cells in vitro by dipyridamole, Pharm. Res. 9 (1992) 178–181.
[37] C.R. Boyer, P.L. Karjian, G.M. Wahl, M. Pegram, S.T. Neuteboom, Nucleoside transport inhibitors, dipyridamole and p-nitrobenzylthioinosine, selectively potentiate the antitumor activity of NB1011, Anticancer Drugs 13 (2002) 29–36.
[38] M. Rodrigues, F. Barbosa Jr., J.R. Perussi, Dipyridamole increases the cytotoxicity of cisplatin in human larynx cancer cells in vitro, Braz. J. Med. Biol. Res. 37 (2004) 591–599.
[39] N.J. Curtin, K.J. Bowman, R.N. Turner, B. Huang, P.J. Loughlin, A.H. Calvert, B.T. Golding, R.J. Griffin, D.R. Newell, Potentiation of the cytotoxicity of thymidylate synthase (TS) inhibitors by dipyridamole analogues with reduced alpha1-acid glycoprotein binding, Br. J. Cancer 80 (1999) 1738–1746.
[40] A.H. Bacelar, M.A. Carvalho, M.F. Proença, Synthesis and in vitro evaluation of substituted pyrimido[5,4-*d*]pyrimidines as a novel class of anti-*Mycobacterium tuberculosis* agents, Eur. J. Med. Chem. 45 (2010) 3234–3239.
[41] J.Z. Xing, L. Zhu, J.A. Jackson, S. Gabos, X.J. Sun, X.B. Wang, X. Xu, Dynamic monitoring of cytotoxicity on microelectronic sensors, Chem. Res. Toxicol. 18 (2005) 154–161.
[42] J.Z. Xing, L. Zhu, S. Gabos, L. Xie, Microelectronic cell sensor assay for detection of cytotoxicity and prediction of acute toxicity, Toxicol. in Vitro 20 (2006) 995–1004.
[43] B.K. Lundholt, K.M. Scudder, L. Pagliaro, A simple technique for reducing edge effect in cell-based assays, J. Biomol. Screen. 8 (2003) 566–570.